

Ductile Crack Growth in Surface Cracked Pressure Vessels

Osama A. Terfas, and Abdusalam A. Alaktiwi

Abstract—Pressure vessels are usually operating at temperatures where the conditions of linear elastic fracture mechanics are no longer met because massive plasticity precedes crack propagation. In this work the development of a surface crack in a pressure vessel subject to bending and tension under elastic-plastic fracture mechanics conditions was investigated. Finite element analysis was used to evaluate the hydrostatic stress, the J-integral and crack growth for semi-elliptical surface-breaking cracks. The results showed non-uniform stress triaxiality and crack driving force around the crack front at large deformation levels. Different ductile crack extensions were observed which emphasize the dependent of ductile tearing on crack geometry and type of loading. In bending the crack grew only beneath the surface, and growth was suppressed at the deepest segment. This contrasts to tension where the crack breaks through the thickness with uniform growth along the entire crack front except at the free surface. Current investigations showed that the crack growth developed under linear elastic fracture mechanics conditions will no longer be applicable under ductile tearing scenarios.

Keywords—Bending, ductile tearing, fracture toughness, stress triaxiality, tension.

I. INTRODUCTION

IN the context of realistic defects in engineering structures predictions of crack growth and crack shape development under ductile tearing have yet to be established. This is an issue for defect assessments in engineering components such as pressure vessels where a surface crack may develop through a different sequence of shapes compared with fatigue and stress intensity factor driven failure. The development of the crack shape becomes important when considering the stability of crack growth as well as in a Leak-Before-Break (LBB) methodology[1]-[2]. In LBB applications the crack shape development is important, as this governs the estimate of the crack opening area or leak rate at breakthrough. It is therefore important to investigate the crack shape development under ductile tearing. It is necessary to prove that the crack will breakthrough in a stable mode by fatigue, tearing or creep and that the leak is detected before the fracture instability occurs.

The crack size at detectable-leakage is compared with the critical size and the leak before break is satisfied when the critical size is larger than the detectable leakage crack.

Predictions of the crack growth have been made for fatigue and stress intensity factor driven failure [2]-[7]. Such

calculations show flaw size, shape and a loading mode effects on the subsequent flaw development. For example, in tension dominated geometries surface flaws tend to acquire a near semi-circular profile until the flaw breaks-through the vessel wall [8]. Conversely under bending dominant loading the flaw evolution is more complex and is a competition between the extension through the thickness and growth on the surface. However a preferred shape through decrease in the a/c ratio (a -the crack depth, c -the major length at surface) as the crack advances is adopted regardless of the original crack shape. [2] showed that under bending the crack grows more rapidly at the free surface than at the deepest point under sub-critical crack propagation (i.e. fatigue). It also showed the crack does not change its shape for short surface cracks, while the crack grows mainly at the deepest point for longer cracks in tension.

Under ductile tearing, [2] showed the maximum J-integral occurs near to the free surface and decreased towards the deepest points in deep semi-elliptical surface cracks in tension. [9] studied stress triaxiality and plastic deformation in deep semi-elliptical surface cracks and observed non-uniform values under tension. The crack grows the most at the deepest segment on the crack front and the least at the surface. These observations suggest a non-uniform crack growth under ductile tearing conditions, where a surface flaw may develop through a different pattern of shapes to the final through-wall flaw, compared with the stress intensity factor dominated growth. It is therefore important to be able to predict this flaw evolution pattern for flaw evaluations.

II. MATERIAL DATA

The material was taken to be isotropic elastic-perfectly plastic ($n=\infty$) with Young's modulus of 200 GPa, Poisson's ratio of 0.49, and a yield strength of 300 MPa. However in general, non-dimensional results are presented. The material followed the von Mises yield criterion and obeyed an associated flow rule. The notation is based on the cylindrical co-ordinate system shown in Fig. 1.

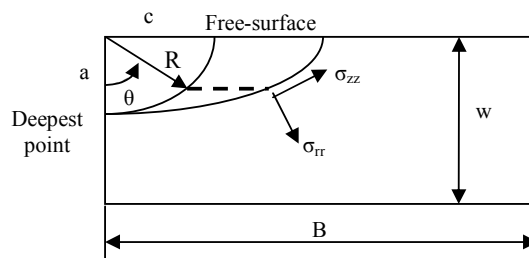


Fig. 1 Illustration of the notation and the cylindrical coordinate system

Osama A. Terfas is with Department of Marine and Offshore Engineering, University of Tripoli, Tripoli, Libya (phone: 00218-91-3184110; e-mail: osamaterfas@tripoliuniv.edu.ly).

Abdusalam A. Alaktiwi is with Department of Marine and Offshore Engineering, University of Tripoli, Tripoli, Libya (e-mail: aktiwi@tripoliuniv.edu.ly).

III. FINITE ELEMENT MODEL

A very refined mesh was used close to the crack front with collapsed three dimensional continuum hexahedral elements C3D8R with coincident but independent nodes were used. The average element size was in the range of $w/1000-2000$ along the crack front, where w is the plate thickness. The elements were biased towards the free surface to accommodate stress gradients. Due to symmetry only one quarter of the geometry was modelled and symmetry boundary conditions were imposed on the appropriate surfaces as shown in Fig. 2.

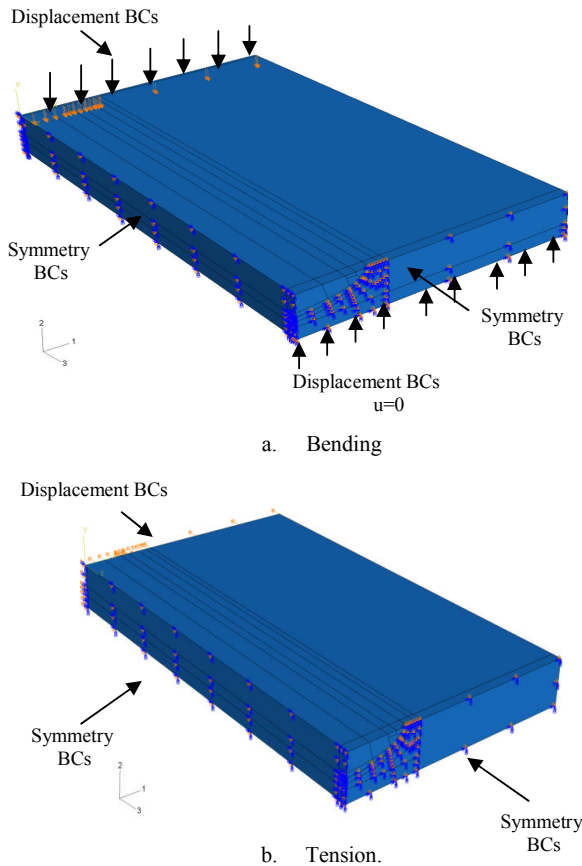


Fig. 2 Quarter model and boundary conditions for elastic-plastic analysis (a) Bending (b) Tension

The load was applied as displacement boundary conditions. The J-integral was evaluated with domain integral technique adopted in ABAQUS using a contour defined in the far field where J-integral is still path-independent. Forty concentric rings of elements were created around the crack tip of a deep semi-elliptical surface crack ($a/w=0.5$, $a/c=0.33$). Each ring contained 300 elements: 30 elements along the crack front and 10 around the half circumference. The total number of elements was 132,153. The mesh is shown in Fig. 3.

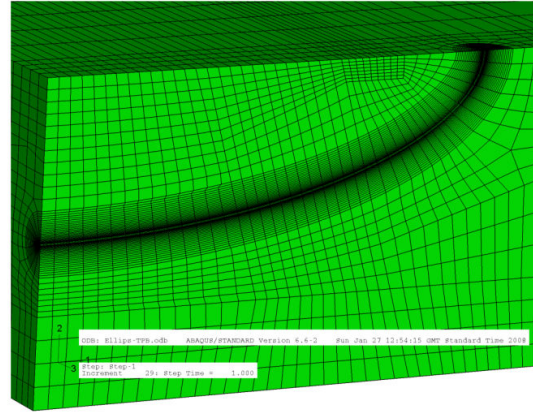


Fig. 3 The mesh for a semi-elliptical surface crack

IV. A PROCEDURE TO DETERMINE DUCTILE CRACK EXTENSION

A procedure developed in [10] to determine the ductile crack extension of semi-circular surface cracks is extended here for different crack geometries and different type of loading. The method is based on experimental ductile tearing resistance curves obtained from plane strain fracture mechanics specimens with a range of crack tip constraints. The resistance curve $J-\Delta a$ depends on the mean stress which for plane strain specimens can be expressed as a function of the T-stress. The $J-\Delta a$ resistance curves in [11] derived from deep and shallow edge cracked bend bars, CTS specimens, centre cracked panels and surface cracked panels shown in Fig. 4 were used as the base data.

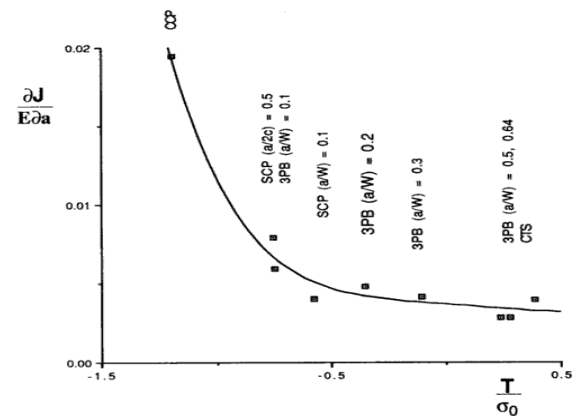


Fig. 4 The slope of the J- Δa resistance curve as a function of T [11]

This data was used to derive a relationship between the mean stress which is a function of the T-stress, and the tearing modulus $T_r = \partial J / \partial \Delta a$. The mean stress can be simply written as a function of the T-stress:

$$\frac{\sigma_m}{\sigma_0} = 2.39 + \frac{T}{\sigma_0} = 2.39 + Q \quad (1)$$

The term ' T/σ_0 ' quantifies the level of constraint at the crack tip in a similar way to the Q-parameter [12]-[13]. The tearing modulus $T_r = (\partial J / (E \partial a))$ derived from Fig. 4 is plotted as a function of the mean stress and is shown in Fig. 5.

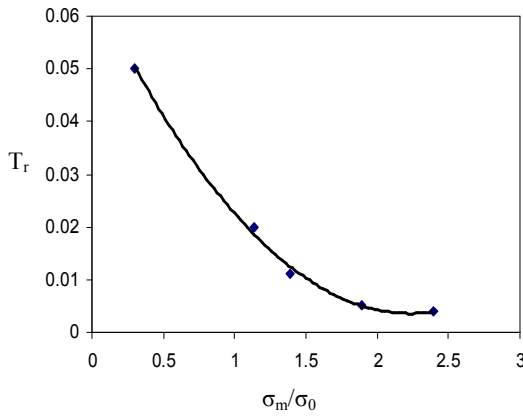


Fig. 5 Tearing modulus as a function of the mean stress

A reduction in the mean stress increases the slope of the J - Δa curve (hence increases the tearing modulus). A curve-fitting procedure gives the relation:

$$T_r = 0.0658 - 0.0557 \left(\frac{\sigma_m}{\sigma_0} \right) + 0.0125 \left(\frac{\sigma_m}{\sigma_0} \right)^2 \quad (2)$$

The tearing modulus is thus taken to be a function of the current level of constraint, but to be independent of deformation level. That is to say the J - Δa curves are taken to be linear. The experimental data in [11] was obtained under plane strain conditions and measured at limited deformation levels, so that constraint is only lost by in-plane effects. However for surface cracked panels it is clear that constraint can be lost by in-plane effects, by proximity to a free surface, and loss of plane strain conditions as well as effects due to the global bending impinging on the near tip field. It is now assumed that the tearing modulus only depends on the current level of mean stress through (2) for all mechanisms of constraint loss.

The applied J to cause a defined amount of crack extension Δa can then be written in terms of the tearing modulus which is a function of the mean stress:

$$J = J_{lc} + \left(\frac{\partial J}{E \partial a} \right) \Delta a E \quad (3)$$

Here it is convenient to define J_{lc} as the applied value of J corresponding to the initiation of crack extension ($\Delta a=0$). This may be contrasted with the definition used in experimental programmes in which it is convenient to define J_{lc} at a small amount of crack extension (i.e. $\Delta a=0.2\text{mm}$). Refer to (3), the crack extension can be in terms of plane strain fracture toughness and the tearing modulus as:

$$\Delta a = \left(\frac{J}{J_{lc}} - 1 \right) \left/ \left(\frac{T_r E}{J_{lc}} \right) \right. \quad J \geq J_{lc} \quad (4)$$

In order to present non-dimensional results the crack extension is normalised on the smallest uncracked ligament, b . Equation (4) can then be re-written in a non-dimensional manner:

$$\frac{\Delta a}{b} = (J - J_{lc}) \frac{1}{T_r E b} \quad \text{For } J \geq J_{lc} \quad (5)$$

Refer to (5) an estimate of the crack extension around the crack front can be made from a knowledge of J_{lc} , the local values of J and the mean stress (at $2J/\sigma_0$) around the crack front, which defines the tearing modulus T_r .

To determine the crack shape pattern associated with continued ductile tearing from surface cracks, the initial crack shape was modelled and analysed for the local J -integral and the mean stress around the crack front. J_{lc} was taken to be $b\sigma_0/100$ so that crack extension occurred in fully plastic conditions. Crack growth was then estimated using (5).

This procedure captures many of the key features of crack extension in surface cracked panels, notably crack extension depends on both the local J value and the local level of constraint. However in order to capture the effects of finite geometry changes a remeshing procedure was introduced. Following the first estimate of crack extension (defined as step zero) a new crack front was created by extending the original crack front by a small increment using (5). The crack growth increment at the point of the maximum growth on the crack front was chosen for convenience. The crack extensions at the other points around the crack front were scaled to be proportional to the extension at this point. A new finite element mesh was then created for each increment of crack growth and the new crack shape was re-analysed for the mean stress and the J -integral. As the material response was idealised as perfectly plastic, strain hardening does not raise the flow stress and the applied load changes only as the geometry changes the limit load. As the tearing-resistance curves are linear the increment ΔJ in each numerical step is related to the increment of local crack extension Δa .

The total value of J at each point around the crack front represents the sum of the increments of J :

$$J = \sum \Delta J \quad (6)$$

Similarly, the total crack extension at each point around the crack front is the sum of the increments of crack extension.

$$a = \sum \Delta a \quad (7)$$

This procedure was used to predict the ductile crack extension and crack shape sequences for surface cracks introduced in a large flat plate subject to bending and tension.

V. RESULTS

A. Deep Semi-Elliptical Surface Cracks ($A/W=0.5$, $A/C=0.33$) in Bending.

1. Crack Tip Stress Field

Fig. 6 shows that plasticity initially developed from the crack at the free surface but was suppressed at the deepest point. The plastic zone also developed from the back face towards the crack front in the uncracked ligament.

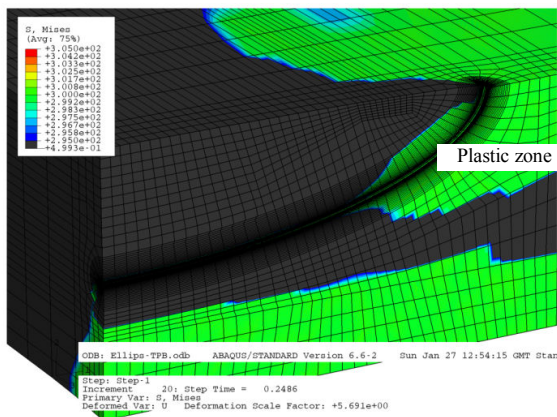


Fig. 6 Development of the plastic zone around a semi-elliptical surface crack ($a/w=0.5$, $a/c=0.33$) at deformation level of $b\sigma_0/J=200$

Fig. 7 shows the mean stress at $2J/\sigma_0$ around the crack front from the deepest point to the free surface. The mean stress reached the highest values at $\theta=0^\circ$ and 22.5° in contained yielding, however as deformation increased ($b\sigma_0/J < 80$) the mean stress reduced to less than 90% of the plane strain HRR value. At 45° a high mean stress was maintained even at high deformation levels ($b\sigma_0/J=60$). At 70° and 77.5° the mean stress reduced significantly with deformation. At the free surface the mean stress exhibited the plane stress value ($0.577\sigma_0$). Fig. 8 shows the largest J-integral occurs at 70° , and the smallest values are located at the deepest point and the free surface.

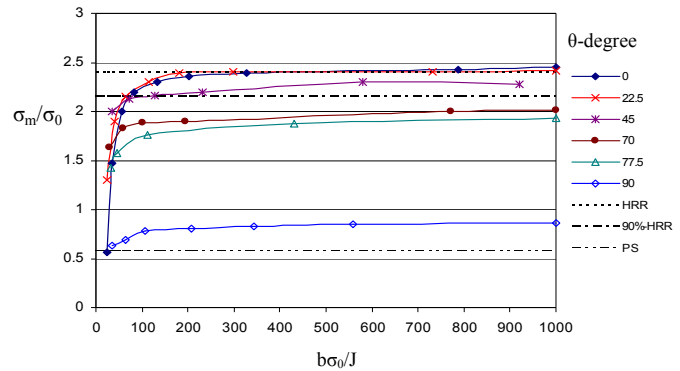


Fig. 7 The mean stress as a function of the level of deformation around the crack at a distance $r\sigma_0/J=2$ for a deep semi-elliptical surface crack ($a/c=0.33$, $a/w=0.5$).

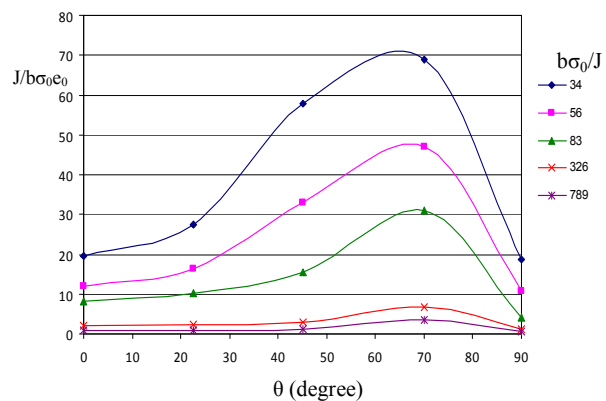


Fig. 8 Non-dimensional J-integral along the crack front in a semi-elliptical surface crack ($a/w=0.5$, $a/c=0.33$) in bending

2. Determination of Crack Growth of a Deep Semi-Elliptical Surface Crack in Bending

Using the J-integral and mean stress with the procedure described in IV the crack extension was determined. Fig. 9 shows the crack growth Δa as a function of the parametric angle (θ). It can be seen that growth occurred with a higher rate at $\theta=45^\circ$ than at the deepest point, where crack growth was suppressed. To establish a crack shape sequence, two more steps were determined after the initial crack extension. Fig. 10 shows that the maximum crack growth for the first and the second steps also occurred at 45° , while crack growth was suppressed at the deepest point and at the free surface, and the crack grew beneath the surface adopting a boat shape.

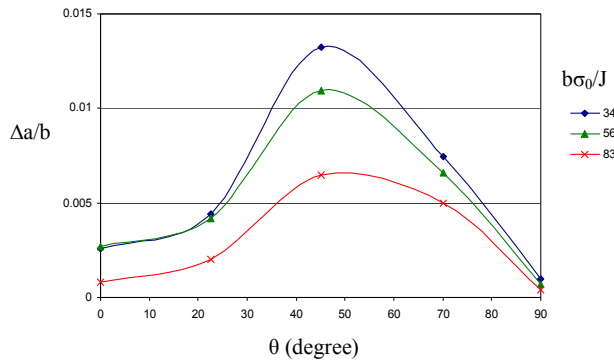


Fig. 9 Crack growth around the crack front as a function of the parametric angle θ for a deep semi-elliptical surface crack in bending



Fig. 10 Crack shape sequence for a deep semi-elliptical surface crack under bending ($a/w=0.5$, $a/c=0.33$)

B. Deep Semi-Elliptical Surface Cracks ($A/W=0.5$, $A/C=0.33$) in Tension.

1. Crack Tip Stress Field

This chapter presents detailed finite element analyses of semi-elliptical surface cracks subject to displacement controlled tension under elastic-plastic conditions. Different plastic zone profiles were observed under tension compared to bending as shown in Fig. 11. In tension the plastic zone developed along the entire crack front including the deepest point, while in bending it developed significantly between 45° and the surface.

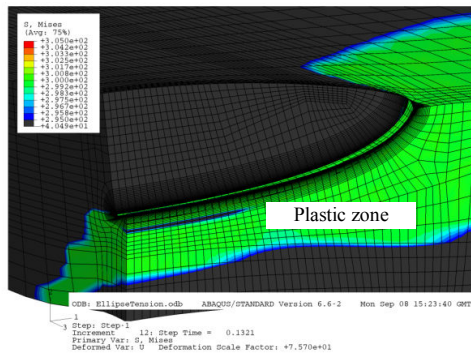


Fig. 11 Development of the plastic zone around the crack for a deep semi-elliptical surface crack in tension, $a/c=0.33$, $a/w=0.5$.

For a deep semi-elliptical crack the largest values of J were located from the deepest point to 45° as shown in Fig. 12. The results in Fig. 13 show that the mean stress is higher from the deepest point to 70° than at the surface.

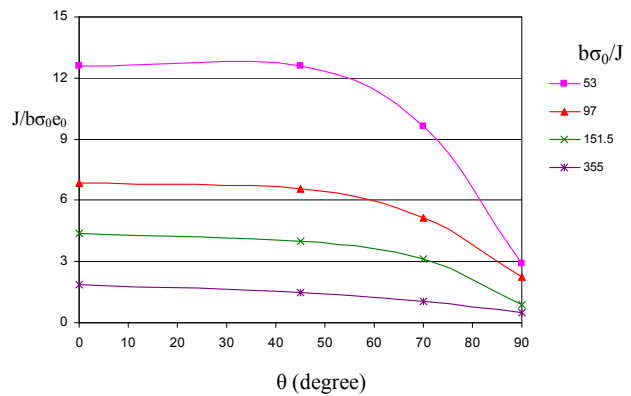


Fig. 12 J-integral along the crack front for a deep semi-elliptical surface crack in tension, $a/c=0.33$, $a/w=0.5$

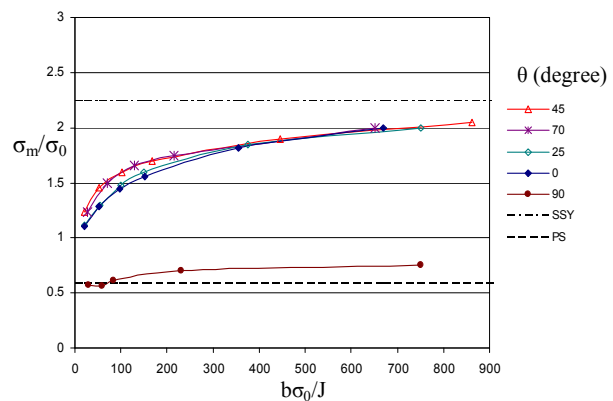


Fig. 13 The mean stress as a function of deformation level along the crack front for a deep semi-elliptical surface crack in tension

The results in Fig. 14 show the crack grows along the entire crack front with more extension at 45° and only a small amount of crack growth at the free surface, where both the J -integral and the mean stress were low. The crack shape sequence showed a uniform crack growth along the crack front until the crack broke through as shown in Fig. 15. This is due to the uniform distribution of the J -integral and the mean stress from the deepest point to 70° . The crack shape sequence is different to bending when crack growth was suppressed at the deepest point and growth only occurred under the surface.

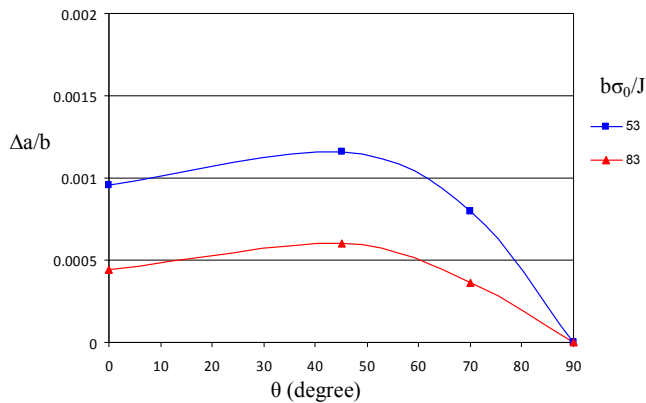


Fig. 14 Crack growth around the crack front as a function of the parametric angle (θ) in a deep semi-elliptical surface crack in tension, $a/c=0.33$, $a/w=0.5$



Fig. 15 The crack shape development for a deep semi-elliptical surface crack $a/c=0.33$, $a/w=0.5$ under ductile tearing in tension

VI. DISCUSSION

Deep semi-elliptical surface cracks in bending initially exhibited a highly constrained stress field under small scale yielding conditions at the deepest point; however the constraint was lost in full plasticity. The loss of a single parameter characterisation (J-dominance) occurred at deformation levels of $b\sigma_0/J=100$. The loss of J-dominance could be due to the effect of the compressive force that dominated the ligament at the deepest point in full plasticity. The largest mean stresses under small scale yielding conditions occurred at the deepest point and decreased gradually towards the free surface. In full plasticity ($b\sigma_0/J < 100$) global bending and out-of-plane effects reduced crack tip constraint at the deepest point, and the maximum mean stress occurred at $\theta=45^\circ$. Surface cracks have curved crack fronts that feature big variations in the stress triaxiality and J-integral along the crack front. Therefore the fracture toughness determined from the standard ASTM J-test is generally conservative when apply to components containing surface cracks.

In tension non uniform stress triaxiality and J-integral distribution along the crack front occurred was smaller than the variation in bending. The level of constraint along the crack front was close to the small scale yielding solution at low deformation levels ($b\sigma_0/J > 1000$). The low level of mean stress in contained yielding is due to the loss of in-plane constraint (T/Q). As plasticity increased a further reduction in the mean stress due to an out-of-plane effect was observed.

This indicates the use of the standard fracture toughness obtained on deep bend samples for surface cracks assessment is excessively conservative. This is because surface cracks under tension show significant constraint loss near the crack tip and the margin of safety is expected to increase accordingly. For semi-elliptical surface cracks ($a/c=0.33$) the mean stress at high deformation levels was greatest in the angular range 45° - 70° and a slight reduction at the deepest point was observed. The J-integral maintained high values from the deepest point up to 45° and then decreased towards the free surface. The current results agree with the finding of [9] where more uniform crack growth was observed along the crack front in tension. It is clear that surface cracks exhibit different behaviour under tension compared to bending. In bending the crack extended only in the width direction under the surface adopting a boat shape which agrees with [14] which predicted that the maximum crack growth under pure bending occurs below the surface. In tension, the crack continued to grow at the deepest point until it broke through the wall. However, a different crack growth profile was observed where uniform crack growth occurred along the entire crack front of semi-elliptical surface cracks compared to more crack extension occurred in the angular range 45° - 70° for semi-circular cracks presented in [10].

Crack growth under elastic-plastic conditions was expected to be more complex as the initial crack geometry was not retained after crack advances under ductile tearing. This is a different profile to crack growth under fatigue or elastic conditions where a simple semi-circular shape developed under tension [8]. While in bending a preferred shape through decrease in the a/c ratio (a -the crack depth, c -the major length at surface) as the crack advances is adopted.

VII. CONCLUSION

The distributions of stress triaxiality and J-integral around the crack front at large deformation levels were different from that at small deformation levels. This emphasises that both, the stress triaxiality and the J-integral were geometry and load dependent, and consequently have a strong effect on ductile crack growth. The J-integral alone can not control crack growth and crack tip stress triaxiality must also be accounted for. Deeply surface cracked geometries subjected to bending tended to grow sub-surface developing a boat shape. These results limit the application of leak-before-break arguments for ductile tearing in flaw assessments. This is significant because a vastly different crack sequence develops under ductile tearing condition compared to fatigue. The crack shapes developed under linear elastic fracture mechanics conditions will therefore no longer be applicable under ductile tearing scenarios. It may also be concluded that single-parameter and two parameter crack tip characterisation are not sufficient to describe the stress field at the crack tip of the surface crack since the stress triaxiality varies along the crack front which may not coincide with the variation of the J-integral. Non-uniform crack extension around the crack front was observed which was dependent on the original crack shape and type of loading. Current work provides solutions of the stress

triaxiality and the J-integral for semi-elliptical surface cracks, and identifies the segment around the crack front that has the lowest resistance to ductile tearing and the segment where crack growth is inhibited.

REFERENCES

- [1] W. Brocks, H. Krafka, G. Kunecke, and K. Wobst, "Ductile crack growth of semi-elliptical surface flaws in pressure vessels," *International Journal of Pressure Vessels and Piping*, vol. 43, pp. 301-316, 1990.
- [2] B. Bricksatd, and I. Sattari-Far, "Crack shape development for LBB applications," *Engineering Fracture Mechanics*, vol. 67, pp. 625-646, 2000.
- [3] L. Hodulak, H. Kordisch, S. Kunzelmann, and E. Sommer, "Influence of the load level on the development of part-through cracks," *International Journal of Fracture*, vol. 14, 1978.
- [4] J. C. JR. Newman, and I. S. Raju, "An empirical stress-intensity factor equation for the surface crack," *Engineering fracture mechanics*, vol. 15, pp. 185-192, 1981.
- [5] A. Carpinteri, "Shape change of surface cracks in round bars under cyclic axial loading," *International Journal of Fatigue*, vol. 15, pp. 21-26, 1993.
- [6] X. B. Lin, and R. A. Smith, "Shape evolution of surface cracks in fatigued round bars with a semicircular circumferential notch," *International Journal of Fatigue*, vol. 21, pp. 965-973, 1999.
- [7] X. B. Lin, and R. A. Smith, "Finite element modelling of fatigue crack growth of surface cracked plates, Part II: Crack shape change," *Engineering Fracture Mechanics*, vol. 63, pp. 523-540, 1999.
- [8] P. M. Scott, and T. W. Thorpe, "A critical review of crack tip stress intensity factors for semi-elliptic cracks," *Fatigue of Engineering Materials and Structures*, vol. 4, pp. 291-309, 1981.
- [9] Y. Chen, and S. Lambert, "Numerical modelling of ductile tearing for semi-elliptical surface cracks in wide plates," *International Journal of Pressure Vessels and Piping*, vol. 82, pp. 417-426, 2005.
- [10] O. Terfas, "The effect of stress biaxiality on crack shape development," *Proceedings of WASET 2012 International conference on materials science and engineering*, August 22-23, 2012, Paris, France. 68, pp. 1644-1649.
- [11] J. W. Hancock, W. G. Reuter, and D. M. Parks, "Constraint and toughness parameterised by T", "Constraint effect in fracture". ASTM STP 1171. Philadelphia, pp. 21-40, 1993.
- [12] N. P. O'Dowd, and C. F. Shih, "Family of crack-tip fields characterised by a triaxiality parameter-1". *Structure of fields. Journal of Mechanics and Physics of Solids*, vol. 39, pp. 989-1015, 1991.
- [13] N. P. O'Dowd, and C. F. Shih, "Family of crack-tip fields characterised by a triaxiality parameter-2". *Fracture applications. Journal of Mechanics and Physics of Solids*, vol. 40, pp. 939-963, 1992.
- [14] X. Gao, J. Faleskog, C. F. Shih, and R. H. Dodds, "Ductile tearing in part-through cracks: Experiments and cell-model predictions". *Engineering Fracture Mechanics*, vol. 59, pp. 761-777, 1998.